BioNanoSci.
DOI 10.1007/s12668-016-0385-8

Preparation of the Sm^{3+}-Doped Magnetic Nanoparticles via Microwave-Assisted Polyol Synthesis

T. A. Lastovina [1] · S. A. Efimova [1] · E. A. Kudryavtsev [2] · A. V. Soldatov [1]

Abstract Sm^{3+}-doped magnetic nanoparticles (NPs) were prepared via microwave-assisted polyol synthesis in ethylene glycol, poly(ethylene glycol) and mixed ethylene glycol—poly(ethylene glycol) solutions. In present work, the effects of organic solvent composition on particle size, particle size distribution, extent of agglomeration, and samarium content in prepared NPs were studied. The synthesized NPs were characterized by several techniques as follows: X-ray diffraction (XRD), transmission electron microscopy (TEM), thermogravimetry (TGA) and X-Ray fluorescence (XRF) analysis. XRD and TEM results showed formation of ~6.0–17.9 nm NPs having different microstructure characteristics (average particle size, particle size distribution, and agglomeration). The TGA analysis indicated the presence of organic components on the surface of NPs. Cytotoxic activity of the prepared magnetic NPs towards HeLa cells was evaluated by using standard live/dead assay in comparison to a control solution. It was shown that prepared magnetic NPs are characterized by low toxicity that makes possible their use for biomedical applications.

Keywords Magnetic nanoparticles · HeLa cells · Polyol synthesis · Microwave-assisted synthesis · Samarium-doped nanoparticles · Iron oxide nanoparticles

✉ T. A. Lastovina
lastovina@sfedu.ru

[1] International Research Center "Smart materials", Southern Federal University, 5, Zorge St, Rostov-on-Don 344090, Russia

[2] Joint Research Center "Diagnostics of structure and properties of nanomaterials", Belgorod National Research University, 85, Pobedy St, Belgorod 308015, Russia

1 Introduction

Due to their unique properties including high magnetic sensitivity, non-toxicity, and biocompatibility iron oxides NPs have been widely used in different biomedical applications [1] such as drug delivery [2], magnetic resonance imaging (MRI) contrast agents [3], cell labeling [4], theranostics [5]. Magnetite (Fe_3O_4) and maghemite (γ-Fe_2O_3) are most widely used among different types of ferromagnetic NPs [6]. Magnetite is a combined Fe^{2+} and Fe^{3+} oxide with 1:2 ratio, which has an inverse spinel structure consisting of octahedral and mixed tetrahedral/octahedral layers stacked along the [111] plane where Fe^{3+} occupy tetrahedral positions and both Fe^{2+} and Fe^{3+} are sited in octahedral ones [7, 8]. Maghemite has a cubic structure and can be considered as fully oxidized magnetite [9]. Substitution of Fe^{3+} by doping with rare earth elements can enhance magnetic properties and increase their resistance to oxidation [10].

Major efforts have been devoted to the synthesis of iron oxides NPs by using co-precipitation [11], microwave-assisted [12], solvothermal [13], electrochemical [14] synthesis, micro-emulsions [15] and high-temperature Fe-containing organic compounds decomposition [16]. One of the promising methods for NPs preparation is polyol synthesis. The polyol technique was developed in 1980s by Fernand Fievet's group for the preparation of fine, highly pure, monodisperse, non-agglomerated metal particles [17, 18]. Polyol process includes three major steps: (1) dissolution of the powdered inorganic metallic precursor in a liquid polyol (ethylene glycol, diethylene glycol, triethylene glycol, propylene glycol, etc., or a mixture of few glycols); (2) reduction of the metals ions by the polyol; (3) nucleation of the metallic phase and growth of the individual nuclei [17, 19]. During the procedure polyol can play a triple role as a solvent, a reducing agent and a surfactant [20]. However, frequently various surfactants are used to prevent sintering of the NPs [21]. Polyol synthesis is

Published online: 20 December 2016

environmentally friendly process because the reactions are carried out under closed system conditions with using of low-toxic organic solvents [22, 23]. Among the advantages that this method presents, it should be mentioned that polyol techniques allow controlling the NPs microstructure (size, shape, particle size distributions, strains, etc.) by manipulating the synthesis conditions: nature of polyol, addition of surfactants, temperature, pH, time of reduction reaction [24]. In addition, polyols provide an opportunity to perform the synthesis procedure in combination with other techniques, for example, microwave-assisted [23] or solvothermal [25] methods.

In the present work, we describe a microwave-assisted polyol synthesis of the Sm^{3+}-doped magnetic NPs by using of ethylene glycol, poly(ethylene glycol) and mixed ethylene glycol/poly(ethylene glycol) solutions as polyol. Cytotoxicity test towards HeLa cells showed their viability. This approach for the synthesis can contribute to the development of biocompatible magnetic NPs preparation.

2 Experimental Part

2.1 Materials

Iron(III) chloride ($FeCl_3$, 97%), ethylene glycol (EG, $C_2H_6O_2$, 99%), poly(ethylene glycol) (PEG, $HO-(CH_2-CH_2-O)_n-H$, BioUltra, 200) were purchased from Sigma-Aldrich. Ultra dry samarium chloride ($SmCl_3$, 99.9% (REO)), sodium hydroxide (NaOH, 98%) were supplied from Alfa Aesar. Chemicals and solvents were used without further purification. Deionized (DI) water was obtained at Simplicity UV system.

2.2 Synthesis

In a typical synthesis, $FeCl_3$ (0.4 mmol) and $SmCl_3$ (13 μmol) were completely dissolved in 15 mL of polyol. The total amount of $SmCl_3$ was calculated from the assumption that the molar ratio of Sm^{3+} ions obtained after $SmCl_3$ dissolution to total amount of Fe^{3+} and Sm^{3+} ions being 3.2%. Then, 2.4 mL of EG (or PEG in the case of the synthesis in 100% *v/v* PEG media) containing 2.4 mmol NaOH was added. The solution has been blowing with argon for 10 min to reduce oxygen content. Prepared solution was heated in a MW-reactor (Discover SP, CEM) for 90 min at 220 °C. After the reaction vessel was cooled down to room temperature; a black precipitate was washed several times with DI water, ethanol and again with DI water, and separated by a magnet. Obtained powder was dried in a vacuum oven at 60 °C overnight.

As a polyol reacted as solvent, reduction agent and stabilizer pure EG, PEG, and different mixed solutions were used: 10% *v/v* PEG +90% *v/v* EG, 30% *v/v* PEG +70% *v/v* EG, 50% *v/v* PEG +50% *v/v* EG, 70% *v/v* PEG +30% *v/v* EG.

2.3 Characterization of the Synthesized NPs

XRD patterns were collected with Ultima IV powder diffractometer (Rigaku) using Cu Kα radiation (α = 1.5406 Å) with

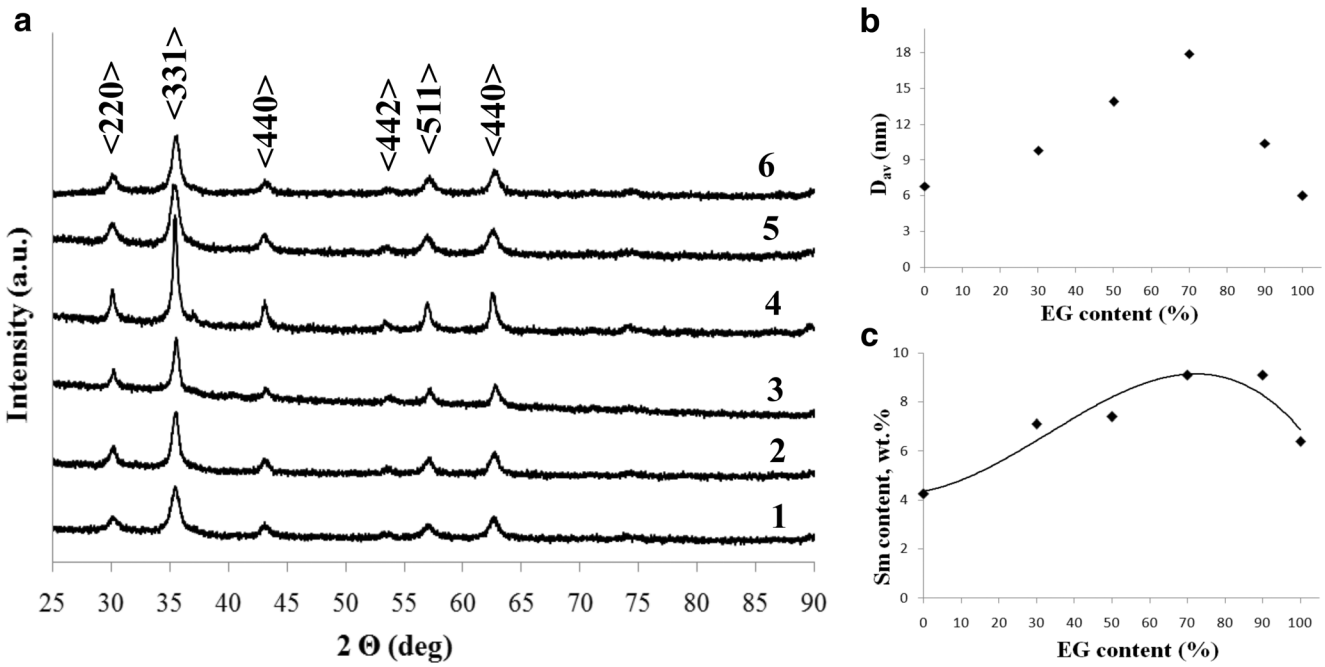

Fig. 1 XRD **a** patterns of Fe_3O_4 NPs prepared in different organic solvents: *1* 100% EG, *2* 90% *v/v* EG + 10% *v/v* PEG, *3* 70% *v/v* EG + 30% *v/v* PEG, *4* 50% *v/v* EG + 50% *v/v* PEG, *5* 30% *v/v* EG + 70% *v/v* PEG, *6* 100% PEG, dependence of the average particle size on the EG content (**b**) and dependence of the Sm concentration on the EG content (**c**)

Table 1 Average particle size calculated from XRD results and samarium content

Solution composition	D_{av} [XRD] (nm)	Lattice parameter (A)	Sm content (wt.%)
100% EG	6.0	8.401	6.4
90% *v*/*v* EG + 10% *v*/*v* PEG	10.4	8.385	9.1
70% *v*/*v* EG + 30% *v*/*v* PEG	17.9	8.383	9.1
50% *v*/*v* EG + 50% *v*/*v* PEG	13.9	8.399	7.4
30% *v*/*v* EG + 70% *v*/*v* PEG	9.8	8.396	7.1
100% PEG	6.8	8.369	4.25

a 0.02° 2θ step size and a 2-s dwell time from 25° to 90° of 2θ. Operating power was 40 kV and 40 mA.

TEM images were acquired on JEM-2100 microscope (JEOL) operated at an accelerating voltage of 200 kV.

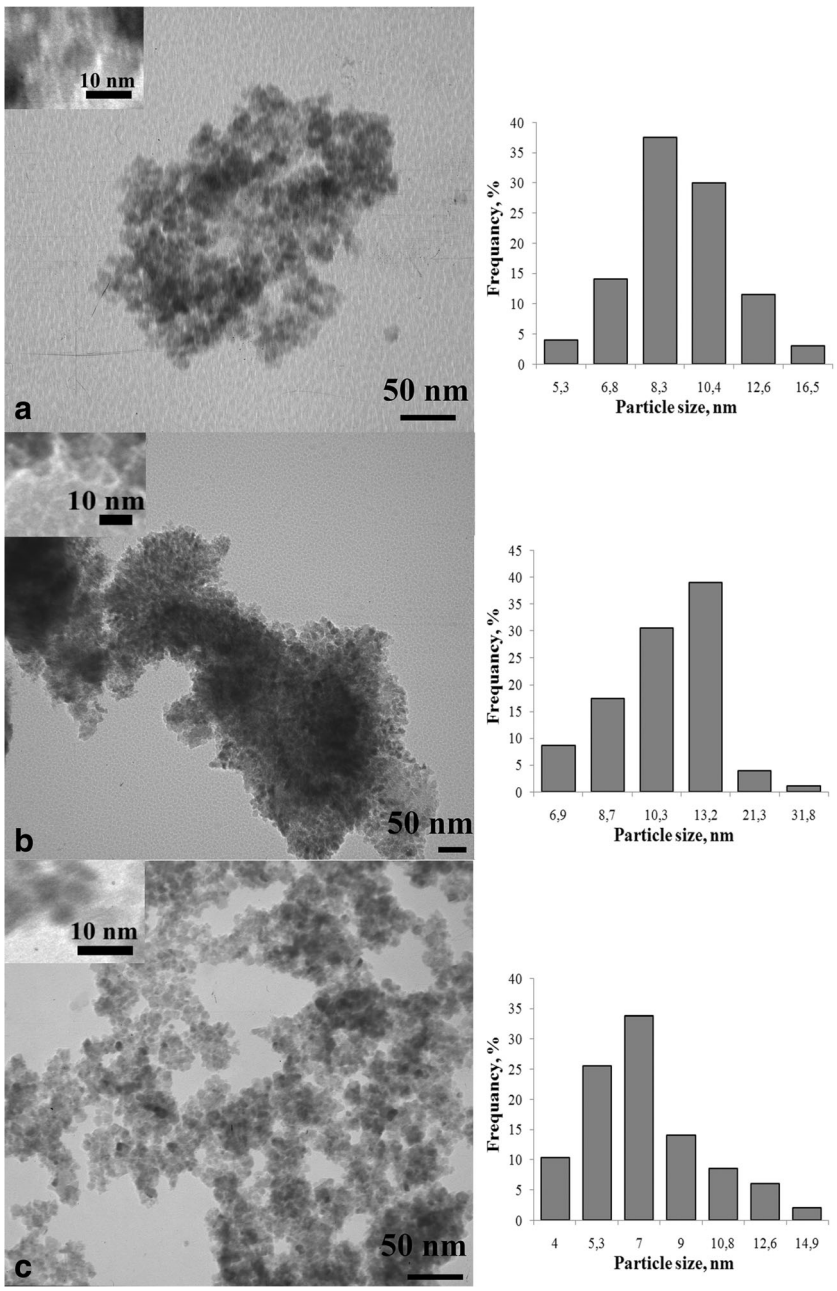

Fig. 2 TEM image, magnification of the particles and particle size distribution histogram for the NPs prepared from **a** 100% EG solution, **b** 50% *v*/*v* EG + 50% *v*/*v* PEG solution, **c** 100% PEG solution

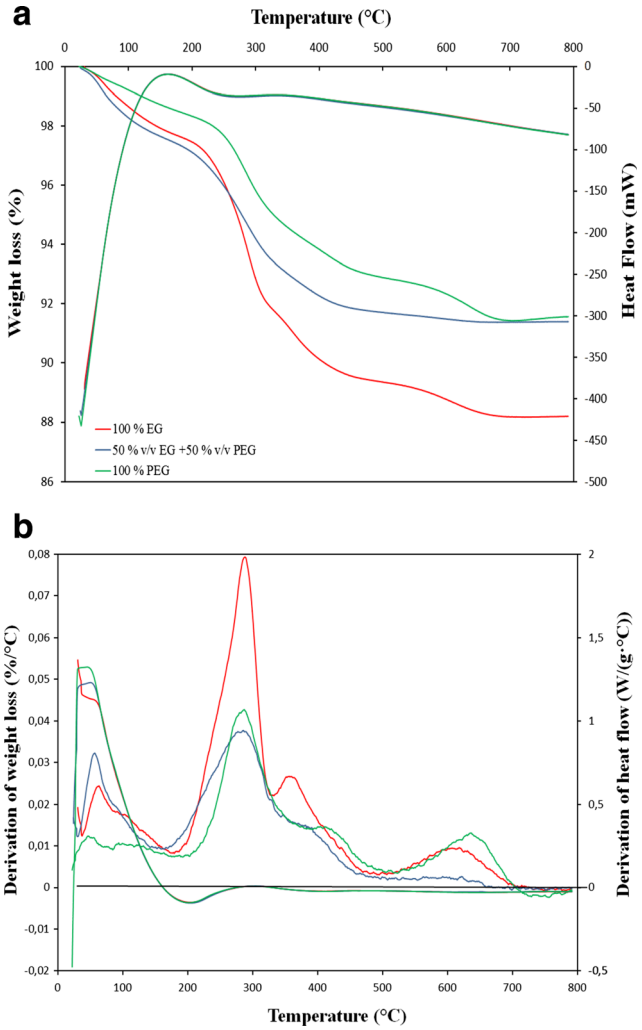

Fig. 3 TGA (**a**) and DSC (**b**) curves of the materials prepared in 100% EG, 50% *v/v* EG + 50% *v/v* PEG, and 100% PEG solutions

Thermogravimetric analysis (TGA) and differential scanning calorimetry (DSC) of samples were performed using a SDT Q600TGA/DSC/DTA thermal analyzer. Samples were heated from room temperature to 800 °C at 10 °C/min rate under argon flow.

Elemental analysis (Fe, Sm) was carried out on M4 TORNADO Micro-XRF spectrometer (Bruker). The sample powder was deposited on a surface of pressed boric acid disk.

Magnetic susceptibility measurements were performed with a vibrating sample magnetometer (VSM) (Lake Shore VSM 7400, USA) in the magnetic field range from −19,000 to 19,000 Oe at room temperature.

We used HeLa cell line as the cell model for toxicity tests. The cells were subcultured in T25 flasks, and further cultured for analysis in 96-well plates (SPL Lifesciences, South Korea) in the GlutaMax DMEM medium (Thermo Fisher Scientific, USA) supplemented with 10% of fetal bovine serum (GE Healthcare, UK) and 0.05 μg/ml of gentamicin (Biokhimik JSC, Russia). The cells were kept at 37 °C and 5% CO_2, with passive humidification in the Sanyo MCO-18 AC incubator (Panasonic, Japan).

For cell viability assay, the nanoparticle formulations were resuspended in physiological saline so as to reach final culture medium concentration of 50 or 25 μg/mL. Cell viability was assessed using the trypan blue exclusion assay in three different days, two biological replicates per day, two technical replicates per biological replicate for each nanoparticle sample. Briefly, the 30,000–40,000 cells treated with the nanoparticle formulations and control saline were detached with 0.25% trypsin-EDTA solution and mixed with equal volume of 0.4% trypan blue (Thermo Fisher Scientific, USA) and, after 2 min of incubation, counted in the Goryaev chamber (the chamber is analogous to the hemocytometer; Minimed LLC, Russia) under a PrimoStar microscope (Carl Zeiss, Germany). There were about 500 cells under a microscopic examination.

Cell viability data are presented as mean ± SD. The data were analyzed for normality (the zero hypothesis was retained in all cases) using Kolmogorov-Smirnov test and for statistical

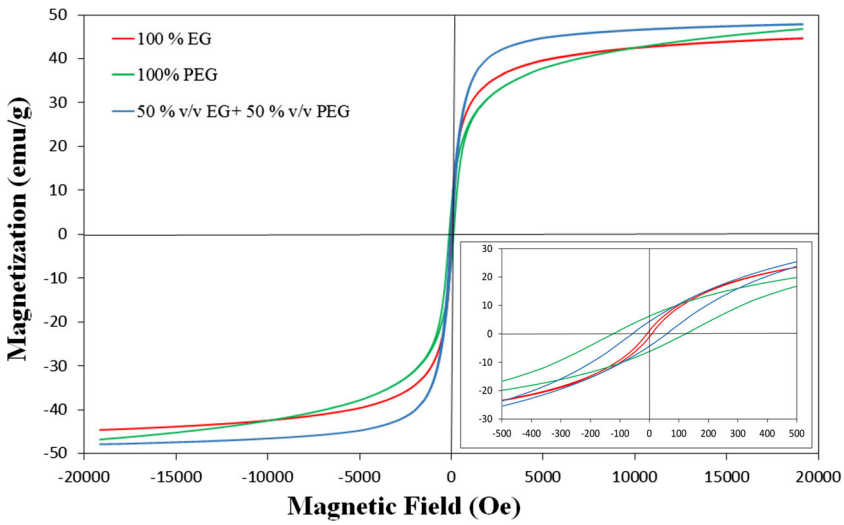

Fig. 4 Magnetization curves of the materials prepared in 100% EG, 50% *v/v* EG + 50% *v/v* PEG, and 100% PEG solutions

Table 2 Magnetic characteristics of the prepared materials

Sample	Coercivity, H_c (Oe)	Magnetization, M_s (emu/g)	Remanence, M_r (emu/g)
100% EG	10	44.6	1.1
50% *v*/*v* EG + 50% *v*/*v* PEG	60	47.8	4.3
100% PEG	150	46.8	6.2

differences using both non-parametric Mann-Whitney test and parametric ANOVA. The tests were cross-consistent. Statistical calculations were performed using the SPSS 22 package.

3 Results and Discussion

The XRD patterns for all samples are given in Fig. 1a. The observed reflexes at 2θ degrees of 30, 35.4, 43.3, 53.6, 57.0, and 62.6 indicated about a cubic spinel structure formation. The average particle sizes calculated by Williamson-Hall method are presented in Table 1.

It can be seen that average particle size depend on the solution composition (Fig. 1b, Table 1). The biggest particles were prepared in the 70% *v*/*v* EG + 30% *v*/*v* PEG and 50% *v*/*v* EG + 50% *v*/*v* PEG solutions. On the other hand, the influence of another solvent on composition is not such significant and allow preparing similar small particles 6.0–10.4 nm in size. Moreover, samarium content depends on solvent composition. With increasing of PEG concentration in solvent during synthesis samarium content in the prepared NPs at the first stage enhances and then, when the concentration of PEG is bigger than 30 *v*/*v* %, slowly reduces (Fig.1c, Table 1).

Results obtained from TEM indicated the formation of big agglomerates with broad particle size distribution in the case of NPs prepared from EG (Fig. 2a) and 50% *v*/*v* EG + 50% *v*/*v* PEG (Fig. 2b) solutions. In contrast, synthesis in PEG solution results in the formation of small well-defined NPs (Fig. 2c) with narrow particle size distribution. Also, it can be noted that synthesis in pure EG solution results in the formation of homogeneous NPs with uniform spherical shape. It can indicate that PEG is more efficient stabilizing agent for such synthesis conditions.

Moreover, the average particle size values calculated from XRD and TEM data for the NPs prepared in 100% EG and 50% *v*/*v* EG + 50% *v*/*v* PEG solutions are different, whereas size values for the NPs prepared in 100% PEG solution are similar for XRD and TEM results. This can be explained by a variety of reasons. The first, an addition of PEG reduces the solvent's viscosity and may affect the nucleation of NPs. Moreover, PEG differs from EG in boiling point and by reduction activity. As a result, the processes of partial reduction of the Fe^{3+} ions into Fe^{2+} and formation of the magnetite NPs proceed slowly in the solutions with high PEG concentration.

Figure 3 shows the TGA and DSC curves of the samples prepared in 100% EG solution, 50% *v*/*v* EG + 50% *v*/*v* PEG solution and 100% PEG solution. The TG curves consist of three typical stages: ~200–250, ~250–560, and ~560–680 °C. Weight loss below 200 °C can be attributed to the removal of bound water [26] and free organic components from the surface of NPs [27]. The next stage beginning at about 250 °C can be related to the decomposition of the organic components directly bent with magnetic NPs. According to the literature data, small weight loss in the range of ~560–680 °C can be explained by phase transition from Fe_3O_4 to FeO, because FeO is thermodynamically stable above ~570 °C in phase diagram of the Fe–O system [28, 29] according to the following Eq. [29]:

$$Fe_3O_4 \xrightarrow{\Delta,\ -1/2\ O_2} 3FeO \quad (1)$$

The quantities of the residue after thermal degradation of the samples prepared in 100% EG solution, 50% *v*/*v* EG +

Table 3 Results of iron oxide NPs cytotoxicity test towards HeLa cell line

Sample	Test solution (μg/mL)	Number of samples	Cell viability (proportion ± error of proportion)	MW *p* level; ANOVA *p* level[a]
Control (NaCl)	(0.89%)	10	0.79 ± 0.04	–
NPs from 100% EG solution	25	7	0.81 ± 0.03	0.151; 0.137
	50	6	0.75 ± 0.04	0.062; 0.091
NPs from 100% PEG solution	25	7	0.83 ± 0.05	0.085; 0.060
	50g/mL	6	0.77 ± 0.04	0.301; 0.377

[a] Note: the NPs test solutions are only compared to the control group

50% *v*/*v* PEG solution and 100% PEG solution were 88, 91.4 and 91.6%, respectively. It can be observed that NPs prepared from the solutions with higher PEG concentration are characterized by the smaller percentage of the residual mass and by the higher thermal stability.

Organic coating of NPs could have a significant impact on their biomedical properties. The presence of PEG on the surface of obtained NPs is not a negative factor. PEG is an important biocompatible polymer being often used as a coating agent for the NPs applications in biomedicine [30, 31].

DSC results are in agreement with TGA data about the three steps of thermal decomposition. The first exothermic peak below 100 °C can be associated with the presence of water in the materials. Than second region has two exothermic peaks at ~290 and 365 °C for the material prepared in 100% EG. For the samples 50% *v*/*v* EG + 50% *v*/*v* PEG and 100% PEG solutions the second peak lays at ~420 °C. The occurrence of these two peaks attributed to the boiling and decomposition of the organic molecules. The last peak in DSC is located at ~620–640 °C for all three samples and can be ascribed to the phase transformation of iron oxide.

The magnetic properties of the NPs were investigated by VSM analysis at room temperature (Fig. 4). The presence of hysteresis indicates that these magnetic NPs are typical ferromagnetic materials. The values of the saturation magnetization (M_s), the coercivity (H_c), and remanence (M_r), as defined from the hysteresis loops, are shown in Table 2. It can be noted that saturation magnetization increases with increase of magnetic particle size. The coercivity and remanence values increase with increasing PEG content in solution.

As iron oxide NPs are promising agents for targeted delivery-and-release as well as for theranostics, their own cytotoxicity is unwanted. The presence of organic compounds on the surface of iron oxide can influence on the NPs cytotoxicity. PEG is often used in many medicines administered by the parenteral, topical, ophthalmic, oral and rectal routes [32]. Some drugs (Busuflex®, Vepesid®, Ativan®) contain PEG as excipients. The World Health Organization (WHO) has set an estimated acceptable daily dose of PEGs at up to 10 mg/kg of body weight [33]. Moreover, PEG derivatives can include residual ethylene oxide, 1,4-dioxane, polycyclic aromatic compounds, and heavy metals [34]. EG is more toxic than PEG, as indicated in [35] a tolerable intake of EG is 0.05 mg per kg of body weight per day.

The main benefits of using iron oxide NPs are true only when their enhanced permeability and retention (EPR) effect is coupled with capability to be locally activated by ultrasound, magnetic impulses, and heat. The EPR effect is never absolute: the particles will always be distributed over the body to some extent (not many carriers can deliver more than 5% of the injected dose to tumor cells, the rest 95% resulting in normal tissues). Thus, the lower the inherent cytotoxicity of the iron oxide NPs, the better. What is more, better iron oxide NPs are those activated as easy as possible, and this characteristic depends mostly on their magnetic properties.

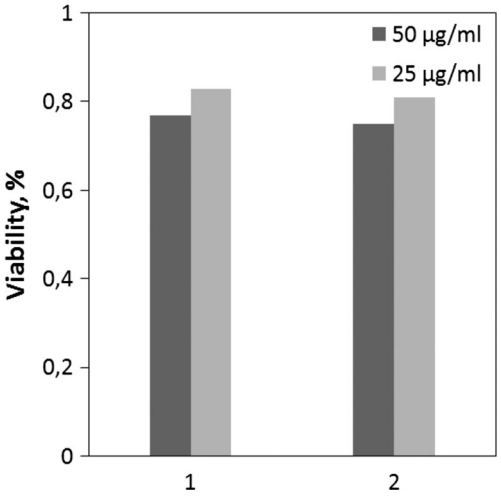

Fig. 5 Resulting cell viability of the cell line HeLa after incubation with different concentrations of iron oxide NPs prepared *1* in 100% PEG solution, *2* in 100% EG solution compared to control (0.89%) sodium chloride solution

The toxicity test for the obtained iron oxide NPs has been performed as a standard evaluation of acute toxicity towards HeLa cells by using live/dead assays. The NPs formulations were resuspended in physiological saline to reach final culture medium concentration of 25 or 50 μg/mL. The averaged viability proportion values are 0.81 and 0.75 for the NPs (in 25 and 50 μg/mL concentrations, respectively) prepared in 100% EG solution, and 0.83 and 0.77 for the NPs prepared from 100% PEG solution (Table 3, Fig. 5).

The results obtained in the solutions with different NPs concentration are the same and indicate about high values of viability. Such results indicated low cytotoxicity of the prepared NPs making them promising for the biomedical application.

4 Conclusions

The present study demonstrates the influence of organic solvent composition on the magnetic NPs particle size, particle size distribution and extent of aggregation. The polyols EG, PEG, and their mixture allow preparing different sizes NPs ranging from 6.0 to 17.9 nm. TEM results indicated formation of small, well-defined spherical NPs with narrow particle size distribution in the case of synthesis in pure PEG. The particles displayed low cytotoxicity towards HeLa cells that makes possible their use for biomedical applications. It can be concluded that microwave-assisted polyol synthesis in EG, PEG, or mixed EG-PEG media results in stable, biocompatible, and nontoxic NPs.

Acknowledgements This study was financially supported by grant of Russian Science Foundation (project no. 14-35-00051).

We thank Dr. Peter V. Zolotukhin and Anna A. Belanova (Evolution corporate group) for assistance with cytotoxicity test, and the Joint Research Center "Diagnostics of structure and properties of nanomaterials" of Belgorod National Research University for TGA and XRD measurements and to Dr. Andriy Budnyk (SFedU) for his contribution during preparation of the manuscript.

References

1. Escamilla-Rivera, V., Uribe-Ramírez, M., González-Pozos, S., et al. (2016). Protein corona acts as a protective shield against Fe_3O_4-PEG inflammation and ROS-induced toxicity in human macrophages. *Toxicol Lett, 240*, 172–184.
2. Mody, V. V., Cox, A., Shah, S., et al. (2014). Magnetic nanoparticle drug delivery systems for targeting tumor. *Appl Nanosci, 4*, 385–392.
3. Zhao, Z., Zhou, Z., Bao, J., et al. (2013). Octapod iron oxide nanoparticles as high-performance T_2 contrast agents for magnetic resonance imaging. *Nat Commun, 4*, 2266. doi:10.1038/ncomms3266.
4. Neoh, K. G., & Kang, E. T. (2012). Surface modification of magnetic nanoparticles for stem cell labeling. *Soft Matter, 8*, 2057–2069.
5. Wang, Y., Jia, H.-Z., & Han, K. (2013). Theranostic magnetic nanoparticles for efficient capture and in situ chemotherapy of circulating tumor cells. *Journal of Materials Chemistry B, 1*, 3344–3352.
6. Gobbo, O. L., Sjaastad, K., & Radomski, M. W. (2015). Magnetic nanoparticles in cancer theranostics. *Theranostics, 5*(11), 1249–1263.
7. Thanh, N. T. K. (2012). *Magnetic nanoparticles: from fabrication to clinical applications*. Boca Raton: CRC Press Taylor and Francis Group.
8. Huang, P. M., Li, Y., & Sumner, M. E. (2011). *Handbook of soil sciences: properties and processes*. Boca Raton: CRC Press.
9. Wu, W., Wu, Z., Yu, T. et al. (2015). Recent progress on magnetic iron oxide nanoparticles: synthesis, surface functional strategies and biomedical applications. *Science and Technology of Advanced Materials*, 16, doi: 10.1088/1468-6996/16/2/023501.
10. Huan, W., Cheng, C., Yang, Y., et al. (2012). A study on the magnetic and photoluminescence properties of Eu^{n+} and Sm^{3+} doped Fe_3O_4 nanoparticles. *J Nanosci Nanotechnol, 12*, 4621–4634.
11. Anbarasu, M., Anandan, M., & Chinnasamy, E. (2015). Synthesis and characterization of polyethylene glycol (PEG) coated Fe_3O_4 nanoparticles by chemical co-precipitation method for biomedical applications. *Spectrochim Acta A Mol Biomol Spectrosc, 135*, 536–539.
12. Garzon-Manjon, A., Solano, E., & de la Mata, M. (2015). Induced shape controllability by tailored precursor design in thermal and microwave-assisted synthesis of Fe_3O_4 nanoparticles. *J Nanopart Res, 17*, 291. doi:10.1007/s11051-015-3070-x.
13. Li, C., Wei, R., Xu, Y., et al. (2014). Synthesis of hexagonal and triangular Fe_3O_4 nanosheets via seed-mediated solvothermal growth. *Nano Res, 7*(4), 536–543.
14. Mazario, E., Sanchez-Marcos, J., & Menendez, N. (2014). One-pot electrochemical synthesis of polydopamine coated magnetite nanoparticles. *RSC Adv, 4*, 48353–48361.
15. Zhang, W., Zhang, H., & Li, D. (2006). Preparation of Fe_3O_4 magnetic fluid by one-step method with microemulsion reactor. *Frontiers of Chemistry in China, 3*, 272–276.
16. Chin, S. F., Pang, S. C., & Tan, C. H. (2011). Green synthesis of magnetite NPs (via thermal decomposition method) with controllable size and shape. *Journal of Materials and Environmental Science, 2*(3), 299–302.
17. Fievet, F., Fievet-Vincent, F., & Lagier, J.-P. (1993). Controlled nucleation and growth of micrometre-size copper particles prepared by the polyol process. *J Mater Chem, 3*(6), 627–632.
18. Rao, C. N. R., Müller, A., & Cheetham, A. K. (2006). *The chemistry of nanomaterials: synthesis, properties and applications*. New York: Wiley.
19. Grisaru, H., Palchik, O., & Gedanken, A. (2003). Microwave-assisted polyol synthesis of $CuInTe_2$ and $CuInSe_2$ nanoparticles. *Inorg Chem, 42*(22), 7148–7155.
20. Abbas, M., Rao, B. P., Naga, S. M., et al. (2013). Synthesis of high magnetization hydrophilic magnetite (Fe_3O_4) nanoparticles in single reaction—Surfactantless polyol process. *Ceram Int, 39*(7), 7605–7611.
21. Coskun, S., Aksoy, B., & Unalan, H. E. (2011). Polyol synthesis of silver nanowires: an extensive parametric study. *Crystal Growth Design, 11*, 4963–4969.
22. Kim, C. W., Cha, H. G., Kim, Y. H., et al. (2009). Surface investigation and magnetic behavior of Co nanoparticles prepared via a surfactant-mediated polyol process. *J Phys Chem C, 113*, 5081–5086.
23. Komarneni, S., Li, D., & Newalkar, B. (2002). Microwave-polyol process for Pt and Ag nanoparticles. *Langmuir, 18*, 5959–5962.
24. Carroll, K. J., Reveles, J. U., & Shultz, M. D. (2011). Preparation of elemental Cu and Ni nanoparticles by the polyol method: an experimental and theoretical approach. *J Phys Chem C, 115*, 2656–2664.
25. Mathur, S., Shen, H., ACer, S., et al. (2010). *Nanostructured materials and systems: ceramic transactions*. New York: Wiley.
26. Xiaoa, W., Gu, H., Li, D., et al. (2012). Microwave-assisted synthesis of magnetite nanoparticles for MR blood pool contrast agents. *J Magn Magn Mater, 324*, 488–494.
27. Mahdavi, M., Ahmad, M. B., & Haron, M. J. (2013). Synthesis, surface modification and characterization of biocompatible magnetic iron oxide nanoparticles for biomedical applications. *Molecules, 18*, 7533–7548.
28. Zhao, S.-Y., Lee, D. K., Kim, C. W., et al. (2006). Synthesis of magnetic nanoparticles of Fe_3O_4 and $CoFe_2O_4$ and their surface modification by surfactant adsorption. *Bull Kor Chem Soc, 27*(2), 237–242.
29. Rahman, O., Mohapatra, S. C., & Ahmad, S. (2012). Fe_3O_4 inverse spinal super paramagnetic nanoparticles. *Mater Chem Phys, 132*, 196–202.
30. Harris, J. M. (2013). *Poly(ethylene glycol) chemistry: biotechnical and biomedical applications*. Berlin: Springer.
31. Jiao, M., Zeng, J., & Jing, L. (2015). Flow synthesis of biocompatible Fe_3O_4 nanoparticles: insight into the effects of residence time, fluid velocity, and tube reactor dimension on particle size distribution. *Chem Mater, 27*(4), 1299–1305.
32. Veronese, F. M. (2009). *PEGylated protein drugs: basic science and clinical applications*. Switzerland: Birkhäuser Verlag.
33. FAO/WHO (1980). Evaluation of certain food additives. Twenty-third report of the joint FAO/WHO expert committee on food additives. World Health Organ Tech. Rep. Ser. No. 648.
34. Fruijtier-Pölloth, C. (2005). Safety assessment on polyethylene glycols (PEGs) and their derivatives as used in cosmetic products. *Toxicology, 214*(1–2), 1–38.
35. World Health Organization (2003). *Ethylene glycol: human health aspects (Concise International Chemical Assessment Documents (Book 45))*.